CONF-781113--1

MATERIALS FOR HIGH-PERFORMANCE LITHIUM ALUMINUM/IRON SULFIDE SECONDARY BATTERIES

BY

R. B. Swaroop, J. A. Smaga and J. E. Battles

Prepared for

V Inter-American Conference on
Materials Technology

Sao Paulo, SP, Brazil

November 5-10, 1978

U of C-AUA-USDOE

ARGONNE NATIONAL LABORATORY, ARGONNE, ILLINOIS

Operated under Contract W-31-109-Eng-38 for the
U. S. DEPARTMENT OF ENERGY

DISCLAIMER

The facilities of Argonne National Laboratory are owned by the United States Government. Under the terms of a contract (W-31-109-Eng-38) between the U. S. Department of Energy, Argonne Universities Association and The University of Chicago, the University employs the staff and operates the Laboratory in accordance with policies and programs formulated, approved and reviewed by the Association.

MEMBERS OF ARGONNE UNIVERSITIES ASSOCIATION

The University of Arizona
Carnegie-Mellon University
Case Western Reserve University
The University of Chicago
University of Cincinnati
Illinois Institute of Technology
University of Illinois
Indiana University
Iowa State University
The University of Iowa
Kansas State University
The University of Kansas
Loyola University
Marquette University
Michigan State University
The University of Michigan
University of Minnesota
University of Missouri
Northwestern University
University of Notre Dame
The Ohio State University
Ohio University
The Pennsylvania State University
Purdue University
Saint Louis University
Southern Illinois University
The University of Texas at Austin
Washington University
Wayne State University
The University of Wisconsin

MATERIALS FOR HIGH-PERFORMANCE LITHIUM ALUMINUM/ IRON SULFIDE SECONDARY BATTERIES

by

R. B. Swaroop, J. A. Smaga, and J. E. Battles
Chemical Engineering Division
Argonne National Laboratory
Argonne, IL 60439

ABSTRACT

Lithium-aluminum/iron sulfide secondary batteries are being developed for use as power sources for electric vehicles and as stationary energy storage devices for load-leveling on electric utilities. The corrosiveness of the active materials and molten electrolyte places severe restrictions on the type of materials that can be used for current collectors, separators, and feedthrough insulators. Out-of-cell and in-cell tests are being conducted to identify the materials that are compatible with this cell environment. This paper discusses the corrosion test procedures, the nature and kinetics of the corrosion reactions, and the development and testing of electrode separators.

I. INTRODUCTION

Lithium-aluminum/iron sulfide secondary batteries with high specific energies (>100 W·h/kg) and high specific power (>100 W/kg) are being developed at Argonne National Laboratory [1] for two major applications: power sources for electric vehicles and energy storage devices for load-leveling on electric utilities. The cells for this battery, which operates at 425-475°C, consist of negative electrodes of lithium-aluminum alloy, positive electrodes of either FeS or FeS_2, and an electrolyte of molten LiCl-KCl (eutectic m.p. 352°C).

The lithium electrode in the high-temperature Li/S cell has been very popular because this electrode promises to yield the highest specific energy of any alkali metal [2]. However, the utilization of both molten lithium and molten sulfur electrodes in a cell employing a molten electrolyte poses difficult engineering problems. The basic problem is containment and separation of the three liquid phases. To circumvent the problems associated with molten electrodes, the solid β-LiAl intermetallic compound was substituted for lithium, and iron sulfide (FeS_2 or FeS) for molten sulfur. The disadvantage of this type of cell is that is has a lower performance (cell voltage, specific energy, and specific power) than the Li/S cell. Although this sacrifice in performance is undesirable, practical Li-Al/MS cells can be fabricated that have lifetime and performance characteristics which meet the requirements of the above applications.

A simplified representation of a Li-Al/FeS_x cell is shown in Fig. 1. The overall reaction that takes place upon discharge can be written as

$$2\ \text{Li-Al} + \text{FeS} \rightarrow \text{Li}_2\text{S} + \text{Fe} + 2\ \text{Al} \qquad (1a)$$

or

$$4\ \text{Li-Al} + \text{FeS}_2 \rightarrow 2\text{Li}_2\text{S} + \text{Fe} + 4\text{Al} \qquad (1b)$$

for cells having FeS and FeS_2 positive electrodes, respectively. The composition of the positive electrode at complete discharge of a stoichiometric cell would be Li_2S and Fe. The Li_2S product dissociates on recharging. Because the active cell materials (lithium, lithium-

aluminum, and iron sulfides) are very reactive at high temperatures, the choices of materials for use in the cell (*i.e.*, insulators, separators, and current collectors) are limited. Accordingly, the selection of materials and the development of low-cost components is a major effort in the development of Li-Al/FeS_x batteries.

Since the corrosive conditions of the negative and positive electrodes are vastly different, candidate materials are corrosion tested for the intended application. Metallic components used in the positive electrode are exposed to various oxidizing metal sulfides. The corrosiveness of the positive electrode environment is further compounded by the anodization of common construction materials (*e.g.*, Al, Ti, Fe, Co, Cu) in the LiCl-KCl electrolyte at potentials less than 2.1 V [3], which is the charge cut-off voltage for cells employing FeS_2 electrodes. For FeS electrodes, the corrosion conditions are less severe because of the lower sulfur activity and a lower charge cut-off potential of 1.65 V. Static corrosion tests (no applied potential) were conducted on metals and on iron- and nickel-base alloys to determine suitable candidate materials for use in the positive electrodes.

Ceramic materials are required for electrode separator and electrical feedthrough insulator applications. Candidate ceramics are evaluated in molten lithium or in mixtures of β-LiAl plus LiCl-KCl electrolyte to determine their compatibility with the highly reducing negative electrode environment which poses the most severe condition for these materials. The final evaluation of all materials is based on in-cell tests of the most promising candidate materials.

The separator for these cells acts as an electrical insulator without unduly restricting ionic flow between the electrodes and as a particle retainer. The separators for these cells must fulfill the following general requirements: low cost, chemically stable in the cell environment, <3 mm thickness and high porosity to minimize cell weight and resistance, mechanical strength to sustain small dimensional changes that occur in the electrodes during operation, and must be wetted by the molten LiCl-KCl electrolyte. Because the BN cloth separators currently used are too expensive, efforts have been directed toward the development of porous felt or loose powder separators. Felt separators are more porous, use less material, and are less expensive than BN cloth separators. The development of powder separators, such as AlN, MgO, β-Si_3N_4, and CaO, is being pursued because separators of this type are amenable to low-cost mass production, and permit the use of materials that are not available in fibrous form.

II. EXPERIMENTAL PROCEDURES

The experimental test procedures for evaluating metallic components, ceramic insulators and separators were as follows:

(a) Metallic Materials

Metallic materials intended for use as current collectors in the positive electrode were evaluated for their compatibility with the positive electrode environment. This environment consisted of an equal volume mixture of LiCl-KCl eutectic and the desired metal sulfide (FeS, FeS_2, $CuFeS_2$, NiS, NiS_2, CoS_2). The disc-shaped samples used in these tests had an initial surface area of approximately 4.25 cm^2. The test samples were inserted into quartz tubes along with the

respective metal sulfide-salt powdered mixture, sealed under a partial vacuum, and then brought to a temperature of 450°C ± 5°C. Two samples of each metallic material were evaluated in each test environment, with half of the samples being tested for 500 h and the remainder for 1000 h. Upon completion of a test, the quartz tubes were cooled to ambient temperature, and the samples were removed from the solidified mixture. The samples were cleaned in water and rinsed with methyl alcohol. Some of the test samples reacted to form a thick, partially adherent reaction layer. This layer was removed for separate analysis, and a determination of the reaction rate was made on the basis of the unreacted base metal.

(b) Ceramic Materials

Candidate ceramic materials intended for insulating and separator applications within the cell were evaluated for their compatibility with the negative electrode environment. A wide range of ceramic materials were screened in molten lithium for 300 h at 500°C. Promising ceramics were further evaluated in molten lithium and then in an equal volume mixture of β-LiAl and LiCl-KCl eutectic for a minimum period of 1000 h at 450°C. The results of tests conducted in β-LiAl and electrolyte are in qualitative agreement with tests in molten lithium, but the rate of attack is accelerated in the lithium tests. These ceramic materials were tested in the following forms: hot-pressed and sintered bodies, felts, cloths, and powders. The experiments were performed in Type 304 stainless steel crucibles. At the end of the testing period, the ceramics were removed from the molten mixture and cleaned in water and rinsed with methyl alcohol. This cleaning procedure removed any adhering electrolyte, lithium or β-LiAl from the sample.

All the corrosion experiments were conducted in a helium glove box to prevent extraneous reactions from occurring between the test environments and/or test materials and the air. The corrosions rates and the nature of the corrosion were determined from gravimetric measurements and microscopic examination. X-ray diffraction and electrode microprobe analyses were also used to identify reaction products and composition changes.

(c) Testing of Electrode Separators

1. Out-of-Cell Tests

The candidates for separator material were characterized by measuring their thickness, porosity, burst strength, flexibility, and wettability. The thickness was measured with an Ames No. 16 Dial Comparator equipped to provide a contact pressure of 862 Pa. The porosity was calculated from measurements of the thickness and weight per unit area of the separator, and from the weight fractions and densities of the component materials. The burst strength of each material was measured on a Mullen Burst Tester Model C.

The wettability of each material by the LiCl-KCl electrolyte was evaluated by the following procedure [4]. The candidate material was first immersed into molten electrolyte (450°C) inside a helium-atmosphere furnace well. If the sample could be infiltrated by the electrolyte without evacuation and repressurization of the helium, the wettability of the material was classified as "good." If evacuation and repressurization with helium was required to wet the material, the wettability was characterized as "fair." If the material was not wet by evacuation and repressurization, the wettability was classified as "poor."

2. In-Cell Tests

Functional tests of the candidate separators were performed in unsealed LiAl/LiCl-KCl/FeS prismatic cells. A schematic of the prismatic test cell is shown in Fig. 1. The cell dimensions were 7.6 x 12.7 x 2.5 cm. The negative electrodes were made of hot-pressed LiAl and LiCl-KCl powder, and the positive electrodes were made of hot-pressed FeS and LiCl-KCl powder. A single positive electrode containing a sheet current collector in the middle was positioned between the facing negative electrodes. The negative and positive electrodes were separated via a separator (felt or powder) contained between two screens. The BN felts used as separators were between 1.25 and 3 mm thick and between 90 and 93 percent porous. These cell were assembled in the 50% charged state in helium glove box and were operated at 450°C in a helium-atmosphere furnace attached to the glove box. The cells were cycled continuously between a discharge cut-off potential of 1.0 V and a charge cut-off potential of 1.65 V (internal cell resistance included). In most of the cells, both charge and discharge current densities were increased in steps of 20 mA/cm^2 from 40 to 120 mA/cm^2 during the first 60 cycles. For the next 40 cycles, the charge current density was held at 40 mA/cm^2 and the discharge current density was held at 40 mA/cm^2 and the discharge current density was again increased in steps of 20 mA/cm^2 from 40 to 120 mA/cm^2, and after approximately 100 cycles the cell was maintained at 40 mA/cm^2 charge and discharge current densities for the rest of the cell lifetime. After termination of cell operation, a post-test examination of the cell and its components was conducted in order to determine the effect and cause of degradation of materials, if any. The examination was generally conducted using an optical microscope, scanning electron microscope, and X-ray diffraction.

For the tests using MgO powder as separator, MgO with a sieve of -60 +120 mesh and a purity of 98% (silica <0.8%) was commercially obtained. The cell design used with the powder separator is essentially the same as that shown in Fig. 1, except that the picture frame and screen assembly was replaced with frames and screens enclosing each negative electrode. The MgO separators used in these test cells had a porosity of 40-50% and a thickness of 0.8-2.0 mm, and were vibratory loaded into the cell. The cell testing procedure was similar to that of the cell using BN felt.

III. RESULTS AND DISCUSSIONS

A. Corrosion Tests and Metallic Components in MS_x Environments

The corrosion resistance of several metallic materials to both the FeS and FeS_2 environments has been investigated [5-8]. These tests were conducted over the 400 to 500°C temperature range, and the results are summarized in Table I.

In the FeS plus LiCl-KCl mixture, the candidate materials, with the exception of Armco Electromagnet iron and AISI 1008 steel, have acceptably low corrosion rates and appear to be suitably corrosion resistant for long-term use in FeS electrodes. Armco iron and low-carbon steel underwent severe intergranular attack, and the resultant grain fallout produced high corrosion rates (> 400 μm/yr) [8]. Low-carbon steel current collectors have been used extensively in engineering-scale FeS cells. The in-cell corrosion rate of this material has averaged 90 μm/yr [8], one fifth the rate determined in static tests. This lower reaction rate is expected, because for a considerable period of time the cell is in the semi-charged and discharged conditions. Under these conditions, the cell is operated at a lower potential and less reactive sulfide species are involved in cell reactions. Nevertheless, with the

present current collector designs for the positive electrode, the effective lifetime of a low-carbon steel collector is approximately one year. Consequently, an alternative material must be selected for use in FeS cells that are going to operate >1 yr. In-cell evaluations are under way for current collectors of nickel- and iron-base alloys to further aid in this selection.

The results of static corrosion tests for metallic materials in FeS_2 plus electrolyte are listed in Table I. For the FeS_2 experiments, molybdenum had an acceptability low rate of less than 20 μm/yr. In tests conducted at or above 450°C, the molybdenum samples showed small weight gains because of the formation of thin (less than 10 μm) layers of weakly adherent MoS_2 [8]. As would be expected from these results, molybdenum has shown superior in-cell corrosion resistance with reaction rates not exceeding 4 μm/yr [8].

Hastelloy B had a marginally acceptable corrosion rate at 400°C of 83 μm/yr, but the corrosion rate rapidly increased to 490 μm/yr at 450°C [5]. The few in-cell corrosion rates determined for this alloy ranged from 190 to 270 μm/yr for cell temperatures of about 450°C [8]. These values are considerably lower than the 450°C rate in static tests but not lower enough to consider Hastelloy B as a viable replacement for molybdenum, which is more costly and more difficult to fabricate. Alternative materials, including other alloys and low cost metals with corrosion-resistant coatings, are being investigated to find more suitable substitutes.

Various metal sulfides have been added to the positive electrode mix to increase cell performance. Recent static corrosion tests were conducted to determine the effects that such additives have on the corrosion resistance of current collector materials. The corrosion rates at 450°C for current collector materials were determined in mixtures of either $CuFeS_2$, NiS, NiS_2, or CoS_2 and LiCl-KCl electrolyte. The corrosion rates are listed in Table II. The rates for these materials in FeS and FeS_2 test mixtures are also included for comparison. For a given test material, the corrosion rates were often an order of magnitude greater in the $CuFeS_2$ and NiS environments than in the FeS environment. Similarly, the tests in the NiS_2 and CoS_2 environments showed a trend toward higher corrosion rates than those determined for the FeS_2 environment. These findings suggest that additions of $CuFeS_2$ or NiS to the FeS positive electrode mix and additions of NiS_2 or CoS_2 to the FeS_2 positive electrode mix can be expected to shorten the effective lifetime of the structural components in the positive electrode.

B. Ceramic Compatibility Test

The results of the compatibility studies on ceramic materials for separator and insulating applications are summarized in Table III [5-8]. Based on the corrosion test results, these materials have been classified into four groups. The first three groups contain materials judged to be incompatible, while the fourth group lists the ceramics found to be compatible with the cell environment.

Ceramics classified in Group I were thermodynamically unstable and readily reacted with the molten lithium. Unstable ceramics, such as SiO_2, and Al_2O_3, underwent complete disintegration during short exposures to the molten lithium. Granules of CaF_2 were somewhat resistant to molten lithium but rapidly

dissolved in the electrolyte. The unstable ceramics of Group II remained intact, but became conductive due to the lithium exposure. Although the net weight losses were small, the stoichiometry of HfO_2 and ZrO_2 was sufficiently altered for these materials to become completely conductive. The lithium attack on these two materials also made them quite friable. Prolonged exposure to molten lithium did not reduce the mechanical integrity of $CaZrO_3$; however, this ceramic developed a conductive surface film [5-7]. Electron microprobe analysis showed that the conductive surface film was partially depleted of zirconium and possibly of oxygen.

The materials in Group III are intrinsically stable to molten lithium; however, these ceramics still failed because of small concentrations of unstable impurities. Silica-rich impurities tend to segregate at the grain boundaries of ceramic bodies. Lithium attack at grain boundaries resulted in the intergranular cracking of Si_3N_4 [9] and the rapid deterioriation of commercial-purity BeO and MgO [8]. Lithium attack on commercially obtained BN resulted in the development of a conductive surface film [6-7]. This reaction was attributed to the presence of the B_2O_3 impurity.

When the impurity levels in inherently stable ceramics are reduced to sufficiently low concentrations these materials are compatible with molten lithium. High-purity beryllia, which is virtually free of SiO_2, exhibited excellent resistance to lithium attack [6]. This grade of BeO is now being used routinely as the lower insulator in the electrical feedthrough assembly of these cells. The conductivity problem associated with the untreated material is eliminated when boron nitride is heat treated at 1700°C in a flowing nitrogen atmosphere to convert or vaporize the B_2O_3 impurity. Boron nitride fabric pretreated by this method has been used successfully in cells operated for more than two years. An MgO single crystal that was tested in molten lithium exhibited only minor weight loss [7]. The intrinsic stability of MgO in crystalline form has been further verified by its successful use as a powder separator in cells such as these discussed in the following section. Other materials tested that showed thermodynamic stability and resistance to lithium attack are AlN, ThO_2, and Y_2O_3.

In conclusion, suitable ceramics for the lithium/metal sulfide cell have been identified. Next, these ceramic components were optimized with respect to cell performance. The progress made in this area is presented in the cell test section.

C. Electrode Separators

The results of the compatibility studies (Table III) have shown that BN, BeO, MgO, Y_2O_3 β-Si_3N_4 and AlN are promising candidates as separator materials. These materials may be used as powder, sintered ceramic plate, fabric, or felt. The fibrous or felt form is available only for Y_2O_3 and BN ceramics. The BN felt developed by the Carborundum Company and Y_2O_3 felt developed by Zircar Products Inc. were characterized for the physical properties before evaluating them for in-cell tests.

1. Physical Characteristics of Felt Separators

The physical and mechanical properties of Y_2O_3 and BN felts are presented in Table IV. The thickness and porosity are useful in evaluating the resistance of the separator to ionic transport and the ability of the separator to prevent the escape of active materials from the electrodes. Thin materials with high porosity

have low resistance to ionic transport; whereas, thick materials with low porosity provide good particle retention of the active material. These data in Table IV indicate that BN and Y_2O_3 felts should allow adequate ionic transport. Flexibility indicates the ease with which the separators can be handled during cell assembly, and the burst strength indicates whether the material can maintain its integrity when dimensional changes occur in the electrodes during cell operation. The BN felt have adequate strength and flexibility to be used in cell construction. At present the BN felt is stabilized at 1750°C for approximately 6 hr in nitrogen to reduce the oxygen content of the felt by vaporizing the residual B_2O_3 (or conversion to BN). The scanning electron micrograph shown in Figure 2 shows that the BN felt consists of long fibers that are bonded at various intersections by the BN bonds. The average size of the openings of the felt is approximately 25 μm and the BN fibers are about 6 μm in diameter.

The wettability is a measure of the facility with which separator becomes penetrated by electrolyte when the cell is filled with electrolyte. The wettability of the two separators is fair for Y_2O_3 felt and poor for BN felt. However, the wettability of BN felt has been improved by treatment with $LiAlCl_4$ [1].

2. In-Cell Testing of Separators

a. BN Felt Separator

In-cell evaluations of separators are conducted to determine materials compatibility, adaptability to cell designs, and the effects of the separator on active material utilization and coulombic efficiency. The active material utilization is the ratio of observed discharged capacity at a given current density to the theoretical capacity. The coulombic efficiency (or A-h efficiency) is the ratio of observed discharged capacity to the charged capacity at a given current density. Figure 3 shows both the coulombic efficiency and utilization for a cell (SC-19) that had a 2.8-mm thick BN felt separator. The utilization decreased from 60 to 35% as the discharge current density was increased in steps of 20 mA/cm^2 from 60 to 120 mA/cm^2 between the 10th and 100th cycles. From cycle 100 to 175, the charge and discharge current densities were maintained at 40 mA/cm^2 and the utilization was steady at 60%. After cycle 175, the cell was thermally cycled to determine the effects of cell freezing on the separator. The cell failed by short circuit after five thermal cycles. During the lifetime of this cell, the coulombic efficiency remained stable at about 99%. Prior to thermal cycling, the utilization of this cell at current densities of 40 mA/cm^2 was about the same (∿62%) as it was during the beginning of operation (between the 15th and 20th cycles). This steady performance indicates that cell components, and especially the BN felt, did not disintegrate during the 3000 hr of cell operation.

Figure 4 shows the effect of separator thickness *vs* utilization as observed from the cells SC-19, 25 and 30. As indicated, utilization was observed to be the best when the separator thickness was the smallest. The utilization decreased as the BN felt thickness was increased. As expected, thicker separators had higher resistance to ionic transport, and hence resulted in decreased cell utilization. Table V gives performance data on three cells using BN felt separators. Even though a marked difference in internal resistance of these cells was not noticed, internal resistance appeared to decrease as the separator thickness decreased. The maximum utilization at a given current

density was observed with the cell using minimum thickness (∿1.25 mm; Cell SC-25) of the BN felt. However, the use of thinner BN felts would require mechanically stronger and denser felts to withstand the internal stresses developed during cell operation. The present results indicate that a cell using BN felt of a thickness between 1.7 and 2.5 mm would produce acceptable performance. Effects on the development and optimization of the physical and mechanical properties BN felts are continuing.

Yttria felt and Y_2O_3 powder cells have been tested successfully [1,4]. However, the further development of Y_2O_3 as a separator material is being abandoned because: (a) Y_2O_3 under long term exposure in the cell environment reacts with sulfur from the positive electrode to form Y_2O_2S [1], and (b) Y_2O_3, if used either as a felt or a powder form still does not meet the cost goal objective of <$22/m^2. The only other materials which would meet this objective are MgO and CaO powder. At present, MgO powder is being evaluated as a separator material.

b. MgO Powder Separator

Magnesium oxide powder separators were tested in Cells SC-21 and SC-28. The performance data for these two cells are given in Table V. The utilization of Cell SC-21 during cycling is presented in Fig. 4. The results indicate that up to a discharge current density of 60 mA/cm^2, the performance of SC-21 was similar to that of the BN felt cells; however, above 60 mA/cm^2, utilization decreased sharply. This is believed to be as a result of the lower porosity of the powder in comparison with the felt separators (∿50 vs 90%) which may restrict ionic transport through the separator at high current densities.

3. Post-Test Examination of Separators and Cells

Operation of some of the cells using MgO powder and BN felts was terminated because of declining performance; operation of the balance of these cells was terminated because the cell testing period had ended. The post-test examinations of these cells indicated that both separator materials are chemically stable in the cell environment. Further, the separator was never a cause of cell failure. Most of the cell failures were caused by short circuits resulting from improper cell assembly, or electrode swelling and subsequent extrusion of active material.

Figures 5a and b show cross-sections of two cells -- SC-26 and SC-19. Cell SC-26 short-circuited within one cycle of operation because of improper filling of the powder separator. In one area, the negative and positive electrode screens were touching each other, thereby causing a short circuit. Cell SC-19 had a gradual decline in performance after 175 cycles because of gradual extrusion of negative electrode into the positive electrode (see Fig. 5b). Figure 5(c) is a photomicrograph of a cross-section of Cell SC-25, which had a gradual decline in performance after 98 cycles. This failure was caused by the presence of fine iron particles from the positive electrode across the felt separator toward the negative electrodes. This behavior was attributed to three factors: (1) the degassing and repressurizing of the cells that is done during operation, (2) inadequate retainment of electrode material by the electrode retaining screens, and (3) overcharging of cells beyond 1.65 V; this causes deposition of iron in the separator. The extrusion of fine

particles from the electrodes can be minimized by the use of active electrode materials which have large initial particle sizes and by the use of fine electrode retaining screens.

IV. CONCLUSIONS

Results have been reported on an extensive materials evaluation program for the selection of suitable low cost ceramic and metallic materials for application in high-temperature, high-energy lithium-aluminum/metal sulfide batteries being developed at Argonne National Laboratory. These materials have been evaluated using static corrosion tests in various environments and in-cell tests. Analysis of the results leads to the following conclusions:

Corrosive attack on a low-carbon steel current collector in an FeS electrode limits its effective lifetime to one to two years. Static corrosion tests indicate that a number of iron- and nickel-base materials are capable of achieving much longer lifetimes. In-cell evaluation of these materials will aid in determining which best optimizes such factors as high corrosion resistance, low electrical resistance, and low cost. For the FeS_2 electrode, none of the alternative materials that have been corrosion tested to date have demonstrated sufficient corrosion resistance to replace molybdenum as the current collector material. The effort to identify a suitable alternative material from the standpoint of cost and ease of fabrication will continue.

Compatibility tests on ceramic materials in molten lithium have shown that several materials: AlN, BN, BeO, MgO, Y_2O_3 and ThO_2 with low impurity concentrations have adequate stability for in-cell applications such as feedthrough insulators and electrode separators.

In-cell tests on BN-felt and MgO powder separators indicate that these separator materials are compatible with the cell environment. At high current densities (>60 mA/cm^2), the cell performance was superior with BN felt separators than with vibratory loaded powder separators. The Y_2O_3 felt separator reacts with sulfur from the positive electrode and formed Y_2O_2S phase; thus Y_2O_3 felt does not appear to be a chemically stable material in the cell environment over a battery lifetime of approximately 5 yrs.

V. ACKNOWLEDGMENTS

The authors wish to acknowledge the administrative support of L. Burris, D. Webster, P. Nelson, D. Barney and R. Steunenberg. A special word of mention is due to F. Mrazek, N. Otto, B. Tani and C. Boquist for assisting us in various ways during the progress of this reported work.

This work is being performed under the auspices of the United States Department of Energy (DOE).

References

1. Nelson, P. A. *et al.*, "High-Performance Batteries for Stationary Energy Storage and Electric Vehicle Propulsion." Progress Reports by Argonne National Laboratory; Report ANL-78-45, ANL-78-21, and ANL-77-75.

2. Cairns, E. J. and Steunenberg, R. K., "High Temperature Batteries," in progress in High Temperature Physics and Chemistry, Rose, C. A. ed. Pergamon Press, New York, (1973), pp. 63-124.

3. Plambeck, J. A., "Electromotive Force Series in Molten Salts," J. Chem. Eng. Data v. 12, p. 77, 1967.

4. Mathers, J. P., Olszanski, T. W., and Battles, J. E., "Evaluation of Porous Paper and Felt Ceramics for Electrode Separators in High Temperature Li-Al/LiCl-KCl/FeS_x Cell," J. of Electrochem. Soc. v. 124, No. 8, p. 1149, 1977.

5. Battles, J. E., "Materials for High Temperature Li-Al/FeS_x Secondary Batteries," in Critical Materials Problems in Energy Production, Stein, C. ed. Academic Press, New York, 1977, pp. 769-804.

6. Battles, J. E., Smaga, J. A., and Myles, K. M., "Materials Requirements for High Performance Secondary Batteries," Met. Transaction A, v. 9A p. 183, 1978.

7. Battles, J. E., Mrazek, F. C., Touhig, W. D., and Myles, K. M., "Materials Corrosion in Molten-Salt Lithium/Sulfur Cells," in Corrosion Problems in Energy Conversion and Generation, Tedmon, C. S. ed. Electrochemical Society, 1974, pp. 20-30.

8. Smaga, J. A., Mrazek, F. C., Myles, K. M., and Battles, J. E., "Materials Requirements in LiAl/LiCl-KCl/FeS_x Secondary Batteries," Paper 111, The International Conference Forum Devoted Exclusively to the Protection and Performance of Materials" organized by NACE, March 6-10, 1978.

9. Singh, R. N., and Touhig, W. D., "Compatibility of Si_3N_4 and Si_3N_4+Al_2O_3 with Liquid Na and Li" v. 58, p. 70, 1975.

Table I

Compatibility* of Metallic Materials with FeS_x/LiCl-KCl Environments over the 400 to 500°C Range

FeS/LiCl-KCl	FeS_2/LiCl-KCl
Compatible:	Compatible:
Molybdenum	Molybdenum
Nickel	Incompatible:
Niobium	Nickel
Type 304 SS	Niobium
Hastelloy B	Type 304 SS
Hastelloy C	Hastelloy B
Inconel 617	Hastelloy C
Inconel 625	Inconel 617
Inconel 706	Inconel 625
Inconel 718	Inconel 706
Incoloy 825	Inconel 718
Incompatible:	Incoley 825
Armco Iron	Armco Iron
AISI 1008	AISI 1008

*Criterion for compatibility is a corrosion rate of less than 100 μm/yr at test temperatures between 400 and 500°C.

Table II

Corrosion Rates for Materials Tested at 450°C
in Various Metal Sulfide Test Environments

Material	Rates in Various MS_x Environments (μm/yr)					
	FeS	$CuFeS_2$	NiS	FeS_2	NiS_2	CoS_2
Molybdenum	3.0	-	-	+1.0	+5.5	+2.8
Hastelloy B	2.5	98	120	490	530	750
Inconel 625	2.7	430	490	1000	1900	>5400
Nickel	+10	1600	2400	>6000	>6000	>6000
Type 304 SS	3.6	4500	2200	>6300	>6300	>6300
AISI 1008	~600	>5000	>5000	>5000	-	-

The corrosion rates listed represent the average value of multiple tests. Those values preceded by a "+" indicate a net weight gain due to the formation of an adherent reaction layer. Those values preceded by a ">" indicate complete reaction of the sample occurred within 500 h.

Table III

Ceramic Compatibility with Molten Lithium

Compatibility Classification	Ceramic
Group I:	
Thermodynamically unstable-excessive attack	Al_2O_3 (sintered) $LiAlO_2$ (sintered) $MgAl_2O_4$ (hot-pressed) SiC (hot-pressed) SiO_2 (fused) CaF_2 (fused grains)
Group II:	
Thermodynamically unstable-intact but conductive	$CaZrO_2$ (hot-pressed) HfO_2 (sintered) ZrO_2 (sintered)
Group III:	
Thermodynamically stable-deleterious concentrations of unstable impurities	BeO (commercial purity) BN (untreated) MgO (hot-pressed) β-Si_3N_4 (hot-pressed or reaction bonded)
Group IV:	
Thermodynamically stable-resistant to attack	AlN (hot-pressed) BeO (high purity) BN (pretreated) MgO (single crystal) ThO_2 (sintered) Y_2O_3 (sintered)

Table IV

Properties of Separator Felts

Property	BN Felt*	Y_2O_3 Felt
Thickness (mm)	1.6	1.75
Porosity (%)	93	96
Basis weight (mg/cm^2)	20	36
Burst strength (kPa)/mm	5-6.5	3-4
Wettability by molten LiCl-KCl	Poor	Fair
Flexibility	Good	Fair
Resistivity (Ω-cm)	4.1×10^{10}	1.3×10^{10}

*Stabilized.

Table V

Separator Test Cells

Cell No.	Separator Type	Separator Thickness mm	Theoretical Capacity	Current Density* at 40 mA/cm^2		Internal Resistance (mΩ)	Operational	
				Percent Utilization (of Active Material)	Specific Energy W-hr/kg		Cycles	Hours
SC-19	BN Felt	2.8	50	62	55	18	205	3050
SC-25	BN Felt	1.25	51	72	66	16	98	1700
SC-27	BN Felt	1.6	48.5	66	59	15	72	1159
SC-30	BN Felt	3.2	48	60	54	18	90	1550
SC-21	MgO Powder	1.8	51	61	55	31	131	1914
SC-28	MgO Powder	0.9	48.5	70	63	20.6	50	982

*Corresponds to 10 hr discharge rate.

Title for Figures

Figure 1: Schematic of Separator Test Cell

Figure 2: Scanning Micrograph of Stabilized BN Felt (500x)

Figure 3: Electrical Performance of Cell SC-19 using BN Felt Separator (2.8 mm)

Figure 4: Utilization Performance of Cells SC-19, 21, 25 and 30.

Figure 5: Post-Test Examinations of Cells SC-26, 19 and 25.

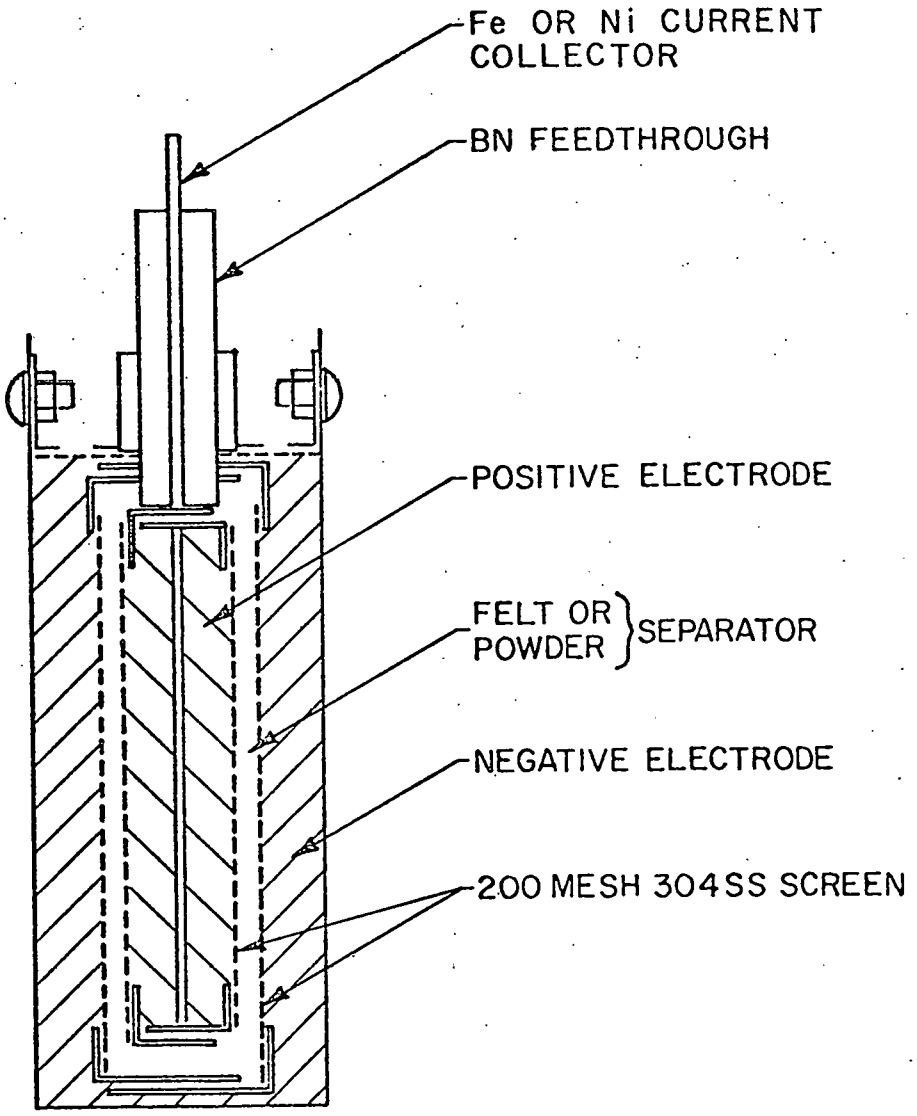
Fe OR Ni CURRENT COLLECTOR
BN FEEDTHROUGH
POSITIVE ELECTRODE
FELT OR POWDER
SEPARATOR
NEGATIVE ELECTRODE
200 MESH 304 SS SCREEN

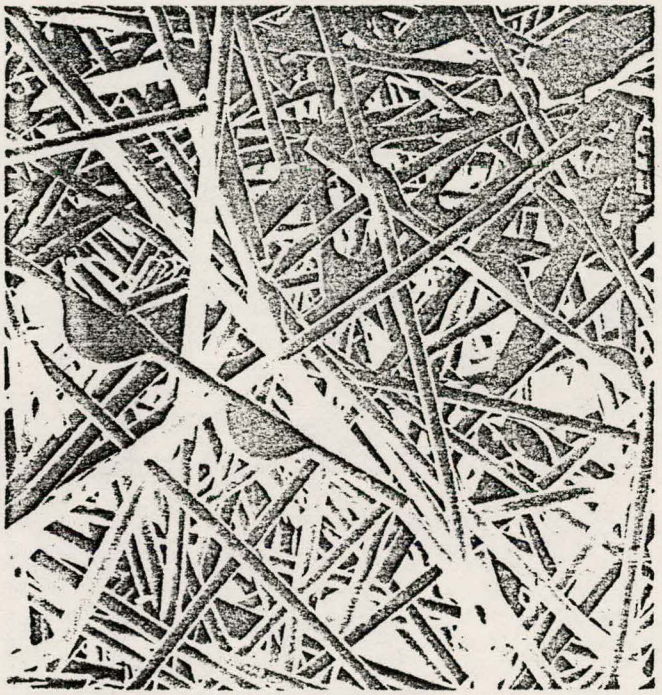

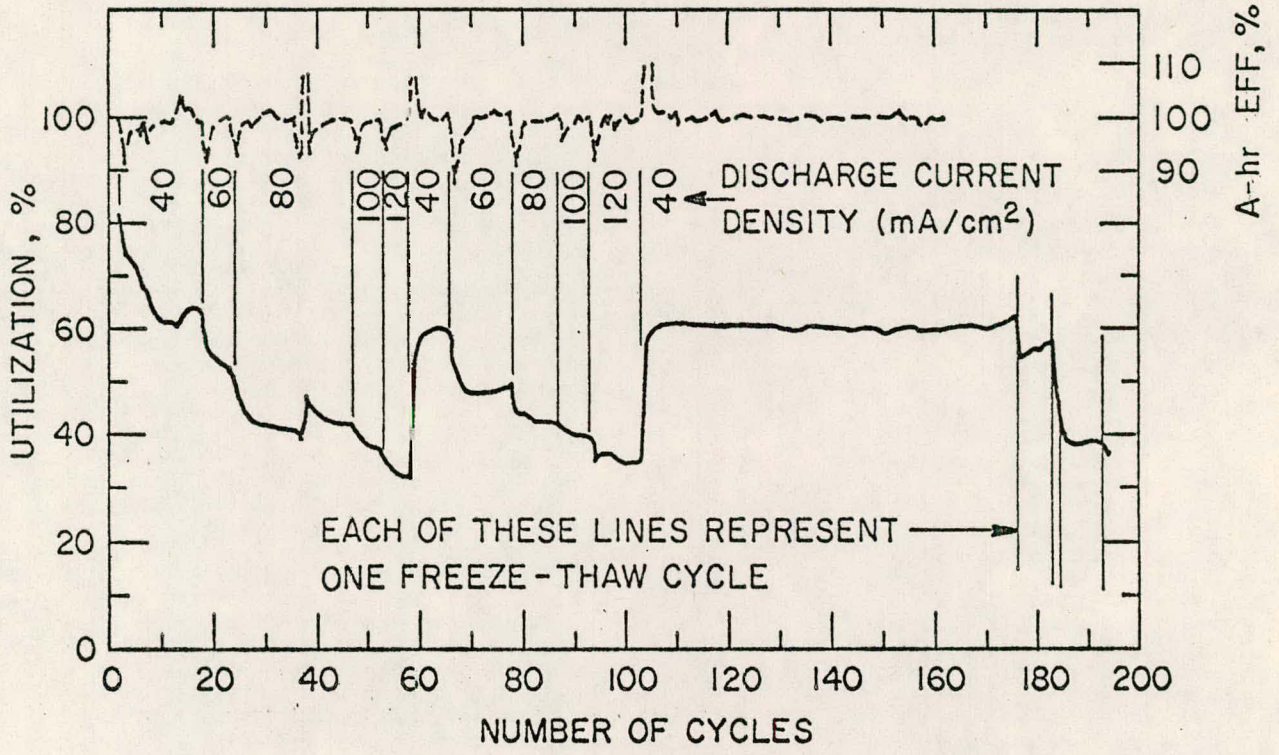
UTILIZATION, %
A-hr EFF, %
NUMBER OF CYCLES
DISCHARGE CURRENT DENSITY (mA/cm²)
EACH OF THESE LINES REPRESENT ONE FREEZE-THAW CYCLE
40
60
80
100
120
40
60
80
100
120
40
0
20
40
60
80
100
120
140
160
180
200
90
100
110

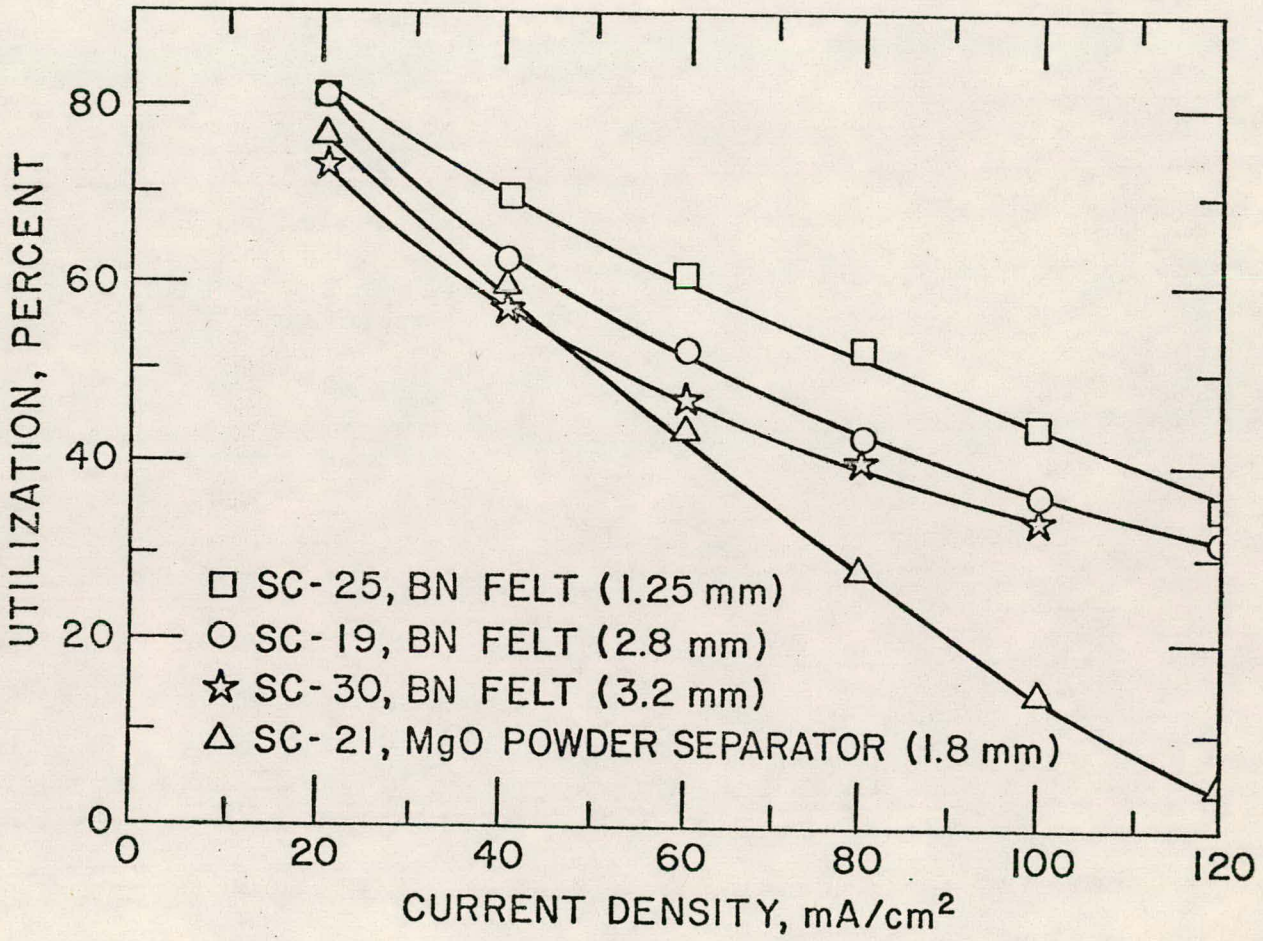
UTILIZATION, PERCENT
0
20
40
60
80
0
20
40
60
80
100
120
CURRENT DENSITY, mA/cm²
□ SC-25, BN FELT (1.25 mm)
○ SC-19, BN FELT (2.8 mm)
☆ SC-30, BN FELT (3.2 mm)
△ SC-21, MgO POWDER SEPARATOR (1.8 mm)

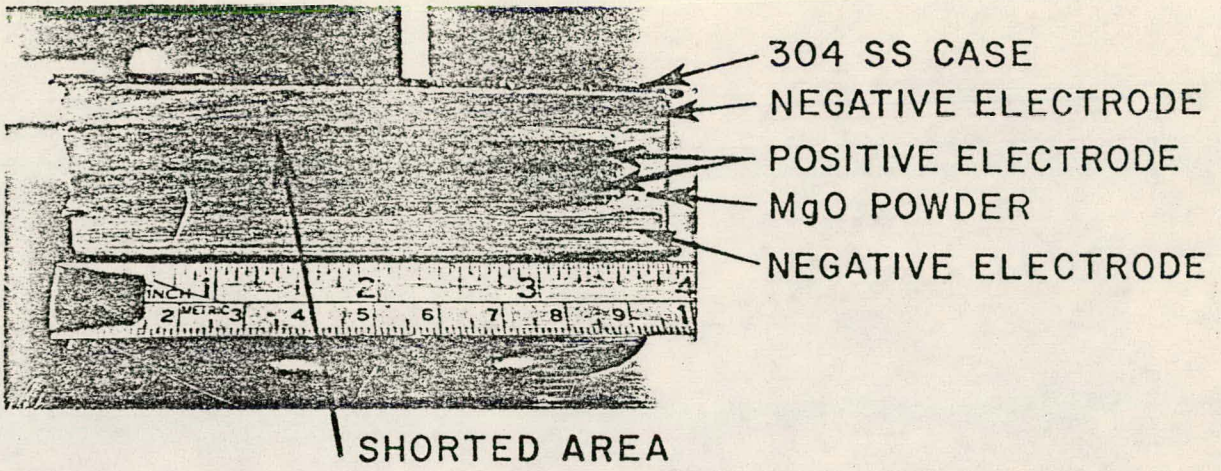

(a) CELL SC-26

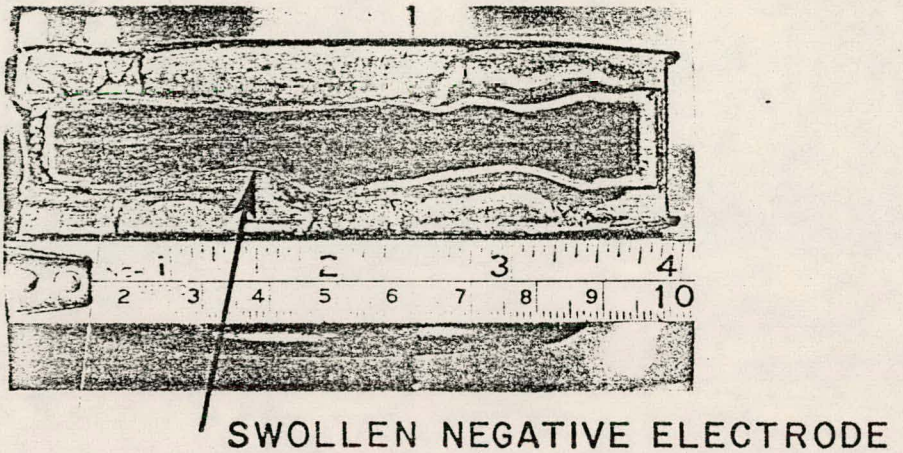

(b) CELL SC-19

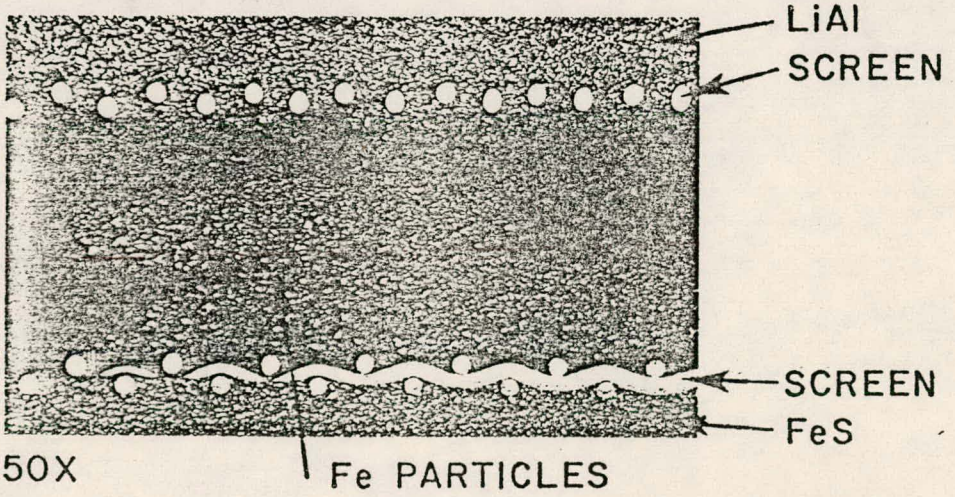

(c) CELL SC-25